

Cite this: *Chem. Sci.*, 2023, 14, 10273 All publication charges for this article have been paid for by the Royal Society of Chemistry

Benchmarking the placement of hydrosulfide in the Hofmeister series using a bambus[6]uril-based ChemFET sensor†

Grace M. Kuhl,‡ Douglas H. Banning,  ‡ Hazel A. Fargher, Willow A. Davis, Madeline M. Howell, Lev N. Zakharov, Michael D. Pluth * and Darren W. Johnson *

Hydrosulfide (HS^-) is the conjugate base of gasotransmitter hydrogen sulfide (H_2S) and is a physiologically-relevant small molecule of great interest in the anion sensing community. However, selective sensing and molecular recognition of HS^- in water remains difficult because, in addition to the diffuse charge and high solvation energy of anions, HS^- is highly nucleophilic and readily oxidizes into other reactive sulfur species. Moreover, the direct placement of HS^- in the Hofmeister series remains unclear. Supramolecular host-guest interactions provide a promising platform on which to recognize and bind hydrosulfide, and characterizing the placement of HS^- in the Hofmeister series would facilitate the future design of selective receptors for this challenging anion. Few examples of supramolecular HS^- binding have been reported, but the Sindelar group reported HS^- binding in water using bambus[6]uril macrocycles in 2018. We used this HS^- binding platform as a starting point to develop a chemically-sensitive field effect transistor (ChemFET) to facilitate assigning HS^- to a specific place in the Hofmeister series. Specifically, we prepared dodeca-*n*-butyl bambus[6]uril and incorporated it into a ChemFET as the HS^- receptor motif. The resultant device provided an amperometric response to HS^- , and we used this device to measure the response of other anions, including SO_4^{2-} , F^- , Cl^- , Br^- , NO_3^- , ClO_4^- , and I^- . Using this response data, we were able to experimentally determine that HS^- lies between Cl^- and Br^- in the Hofmeister series, which matches recent theoretical computational work that predicted a similar placement. Taken together, these results highlight the potential of using molecular recognition coupled with ChemFET architectures to develop new approaches for direct and reversible HS^- detection and measurement in water and further advance our understanding of different recognition approaches for this challenging anion.

Received 13th July 2023
Accepted 2nd September 2023

DOI: 10.1039/d3sc03616b

rsc.li/chemical-science

Introduction

Overview

Hydrosulfide (HS^-) is the conjugate base of the gasotransmitter hydrogen sulfide (H_2S), and is a physiologically-relevant small molecule of emerging interest in the anion sensing community.^{1–10} The selective recognition and detection of HS^- in water, however, remains difficult due to the diffuse charge and high solvation energy of anions in general,⁴ as well as the high nucleophilicity and redox activity of HS^- .⁵ Different detection and quantification methods for H_2S have been reported and typically rely on electrophilic trapping or reaction

with activity-based probes to generate a fluorescent response.^{5,11,12} An alternative approach to activity-based methods that irreversibly couple an H_2S -mediated reaction with an optical response is to use host-guest chemistry to enable reversible $\text{H}_2\text{S}/\text{HS}^-$ detection. Early examples of this approach have included investigations into the ability of hosts to bind HS^- as an anion of interest.^{1–3,6,7,10} A key and unmet need for advancing reversible HS^- detection is a better understanding of the placement of HS^- within the Hofmeister series, which would facilitate the development of receptors with engineered specificity for HS^- over other competing anions. Prior work has described the HS^- position in the Hofmeister series as “unclear”² and “rarely reported.”¹³ Previously, our lab has used chemically-sensitive field effect transistors (ChemFETs) monitor reactive species that are otherwise difficult to characterize. Here we report the translation of a reversible HS^- binding receptor to develop a ChemFET sensor for the hydrosulfide anion. Moreover, we use this system to provide an experimental benchmark for the placement of HS^- in the

Department of Chemistry & Biochemistry, Materials Science Institute, University of Oregon, 97403-1253 Eugene, OR, USA. E-mail: dwj@uoregon.edu; Web: <https://www.dwjlab.com/>

† Electronic supplementary information (ESI) available. See DOI: <https://doi.org/10.1039/d3sc03616b>

‡ These authors contributed equally to this work.



Hofmeister series, which we anticipate can be used to further advance new approaches for selective HS⁻ binding in synthetic receptors.

ChemFET design and response

Electrochemical potentiometric sensors, which incorporate simple instrumentation that is easily integrated with chip-based devices,^{14,15} are one option for HS⁻ detection. Potentiometric sensors interface different membrane designs with sensor components, including inorganic crystal lattices,¹⁶ lipophilic ionophores,¹⁷ or metal–ligand coordination to impart analyte selectivity.^{18,19} The selectivity of an electrochemical sensor is derived from the membrane, and different components that impart selectivity can be incorporated into these membranes. Such components are generally ionophores, which are often either biological or synthetic structures with tailored non-covalent intermolecular interactions, such as hydrogen bonding and related electrostatic forces, that interact selectively with specific analytes.²⁰ Given the well-characterized nature of sensor construction, lipophilic ionophore sensors are therefore a viable option for anion sensing since membrane compositions and properties are well known and easy to process.

ChemFETs have a different internal construction than ion-selective electrodes (ISEs), but they provide a logarithmic potentiometric response to changes in analyte concentration. ChemFETs are useful for aqueous ion sensing due to their fast response, stability, reusability,^{15,20} high signal-to-noise ratios, and low sample volume requirements.²¹ The ChemFET response relies upon the change in potential at the sensing gate, which is covered by an ionophore-doped semi-permeable polymeric membrane to impart selectivity towards the analyte of interest (Fig. 1).

In general, ChemFETs exploit intermolecular interactions (in this case, host–guest interactions between bambusuril and a target anion) to generate a concentration gradient of charged species, which results in a shifting surface potential that impacts a depletion layer between the source and drain terminals.²² This layer allows electrons to flow and a current to be measured, and the magnitude is altered by the field effect and directly relates to the concentration of target analyte in the sample solution.²³



Fig. 1 Chemically sensitive field effect transistor (ChemFET) diagram. For sensor construction, pre-constructed FETs are covered with insulating epoxy, except for the gate nitride/oxide surface, which is coated with the ionophore-containing membranes. Reference electrodes are constructed separately.

ChemFETs are particularly useful to facilitate measurements and characterization of target analytes that are reactive or otherwise difficult to work with. This allows for characterization of species, including assessing the placement of an analyte within the Hofmeister series, that are otherwise inaccessible.

Ionophores for hydrosulfide

Recent work in our labs introduced the first proof-of-concept HS⁻ ChemFET sensor using a nitrile butadiene rubber (NBR) coating and tetraoctylammonium nitrate as a simple lipophilic ionic additive, or ionophore.⁸ Although this approach did not contain a specific receptor for HS⁻, the lipophilic cation yielded modest selectivity for HS⁻ over competing species in water, with selectivity coefficients of 0.12 and 0.13 over Cl⁻ and L-cysteine, respectively. We expected that direct incorporation of a supra-molecular cavitated receptor as a neutral ionophore in a polymer membrane would impart selectivity for aqueous HS⁻ and improve the figures of merit of this device.

When considering available systems for HS⁻ binding^{1,2,6,24} and the above criteria, we chose to use the bambus[6]uril system reported by the Sindelar group in 2018.⁷ Bambus[6]urils contain four or six repeating bicyclic glycoluril units connected by a bridging methylene (Fig. 2).²⁵ These receptors have a defined cavity size, tunable functional groups, and strong anion affinity in water and organic solvents due to strong C–H hydrogen bonding interactions in the cavity.^{25–27} We surmised that integrating a bambus[6]uril receptor into a ChemFET polymer membrane would increase sensitivity and selectivity toward HS⁻. Further supporting this idea, recent work reported a bambus[6]uril based ionophore used to develop a perchlorate-selective ISE-based sensor.²⁸

Hofmeister series

Originally discovered while studying salt effects on protein solubility, Hofmeister effects remain an active area of research in interfacial and host–guest chemistry.^{29,30} The Hofmeister series is an experimentally-derived ranking of ions based on their ability to salt proteins in or out of solution.²⁹ Interestingly, other physical phenomena also follow this same ranking,



Fig. 2 Three-dimensional representation of dodeca-*n*-butyl bambus[6]uril (left). Simplified figure depicting the hourglass-type shape common to bambus[6]urils, with binding pocket depicted in pink highlighting all twelve C–H hydrogen bond donors in the cavity (right). As with the rest of bambus[6]uril family of macrocycles, this receptor is comprised of repeating glycoluril subunits of alternating orientation.



including surface tension and potential.^{29,31} Anions on the chaotropic (or charge diffuse) end of this series, such as ClO_4^- and I^- , increase protein solubility and decrease surface tension and potential, whereas anions on the kosmotropic (or charge dense) end of the series, such as SO_4^{2-} and F^- , increase surface tension and potential while lowering protein solubility (Fig. 3).^{29–32}

Although many of the phenomena that follow the Hofmeister series trend were studied in bulk solution, the Hofmeister trend can also be observed at aqueous interfaces³² such as those found at ISE or ChemFET membranes in an electrolyte solution.³³ The fundamental interactions that influence the Hofmeister effect are not fully understood, but are thought to be a combination of ion size, ion hydration energy, polarization, electrostatics, as well as other phenomena.³¹ Recent work by Page and coworkers used computationally-derived linear charge density of different anions to rank anion positions on the Hofmeister series.³⁴ In potentiometry, the Hofmeister effect is displayed even in the absence of a membrane-bound ionophore, which leads to an even greater sensitivity to chaotropes than kosmotropes.^{35,36}

Results and discussion

Hofmeister series comparison

To investigate whether host incorporation into the ChemFET membrane could be used to place HS^- in the Hofmeister series, we first prepared control sensors without bambusuril ionophore and tested these devices with eight representative anions in the Hofmeister series (Fig. 4). The eight anions were then ranked by detection limit to produce a qualitative Hofmeister-type ranking order. We then performed a second set of experiments under identical conditions, but included the dodeca-*n*-butyl bambusuril ionophore in the gate nitride membrane. This second set of experiments served a twofold purpose: (1) to examine if bambusuril ionophore would increase sensitivity toward HS^- , and (2) to determine whether any re-ordering of anions in reference to the Hofmeister series that would indicate either increasing or decreasing binding preference and selectivity. By comparing these two ChemFET devices we were able to measure the relative affinity and determine whether there was a Hofmeister bias in ion sensitivity in the sensor. In addition to informing on the Hofmeister series, these experiments also inform on the performance of *n*-butyl bambusuril as an HS^- ionophore. Upon incorporation of 1 wt% dodeca-*n*-butyl bambusuril into the PVC-based ChemFET membrane, a lower detection limit was observed for all anions measured, which

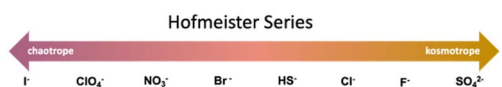


Fig. 3 Common reference anions in the Hofmeister series. This represents a common reference framework for electrochemical sensors. Electrochemical sensors are commonly more sensitive to charge diffuse chaotropes (left) than charge dense kosmotropes (right). In this study, we place HS^- in the series between Cl^- and Br^- (*vide infra*).



Fig. 4 Results of control (no ionophore) sensors in blue, and *n*-butyl bambusuril sensors in orange. A lower detection limit (up on the y-axis) indicates stronger recognition. F^- and Br^- show little difference between control and ionophore-containing sensors, whereas ClO_4^- shows the largest difference. The overall trend shows the most sensitivity to the chaotrope end of the Hofmeister series (I^- and ClO_4^-) and the least sensitivity to the kosmotrope end (SO_4^{2-} and F^-).

supports the importance of the host-guest interaction between the bambusuril ionophore and the anion.

Hofmeister series computations

Initially, the ChemFET sensor runs were intended to provide a qualitative ranking of common anions in a Hofmeister-like series for evaluation of relative affinities. However, the measured detection limits also provide a quantitative means of comparison. One key benefit of using ChemFETs to evaluate anion receptors is that they provide quantitative binding data on highly reactive species within minutes. Recently, Page and coworkers published a Hofmeister series study indicating that theoretical calculation of linear charge density compared very favorably with the experimental placement of anions on the Hofmeister series.³⁴ We were able to use our ChemFET binding data to validate these theoretical computations, including for anions that had not been previously validated experimentally. Specifically, we used the experimentally-derived ChemFET detection limits to place HS^- on the Hofmeister series experimentally. Gratifyingly, this experimental placement of HS^- in the series, specifically between Cl^- and Br^- , matched the theoretical placement by Page (Table 1). Moreover, this placement also corroborates experimental data on $\text{CH}\cdots\text{S}$ interactions that indicate HS^- most closely resembles Cl^- in its binding interactions with related hosts.^{34,37,38} Of particular interest is that the detection limit and binding constant trends mirrored each other.[§]

In addition to the experimental validation of the theoretical Hofmeister placement of hydrosulfide, these results highlight the utility of using electrochemical sensors in this application. ChemFETs appear to be uniquely suited to quickly and efficiently measure Hofmeister trends for highly reactive species that are otherwise unsuitable for other measurement techniques.

Hydrosulfide selectivity

To further investigate whether the ChemFET approach could be used for future HS^- detection, we also evaluated the affinity for



Table 1 Comparison of Page and coworkers' Hofmeister computational data (top box) with ChemFET experimental sensor data (bottom two boxes). Of particular note is one of the only reported Hofmeister series placements of hydrosulfide agrees with the computational placement between bromide and chloride

		I ⁻	ClO ₄ ⁻	NO ₃ ⁻	Br ⁻	HS ⁻	Cl ⁻	F ⁻	SO ₄ ²⁻
Computations (linear charge density, C M ⁻¹)	Theoretical (spherical)	-4.90	-5.53	-6.26	-5.63	-5.68	-6.25	-8.64	-10.25
	Theoretical (polyatomic)		-6.15	-5.78		-6.39			-8.19
No bambusuril (control)	Detection limit (mM)	1.0	6.1	0.83	0.36	15	41	15	78
<i>n</i> -Butyl bambusuril	Detection limit (mM)	0.0078	0.0010	0.057	0.22	0.53	3.6	11	15



Scheme 1 Synthesis of dodeca-*n*-butyl bambus[6]juril (**3**).²⁵

HS⁻ over other competing anions to provide a selectivity coefficient. The selectivity coefficient is calculated *via* a fixed interferent experiment, where the concentration of an interfering anion is kept fixed, and the concentration of target analyte HS⁻ is varied. The concentration at which hydrosulfide is detected above the level of the fixed interferent is used to calculate the selectivity coefficient $K_{A,B}^{\text{pot}}$ using the following equation:

$$K_{A,B}^{\text{pot}} = \frac{a_A}{\frac{z_A/z_B}{a_B}}$$

where a represents the activities of the target analyte A and interferent B at the limit of detection, and z_A and z_B are the respective charges. If $K_{A,B}^{\text{pot}} < 1$, the membrane is selective towards the target analyte A. For example, if the selectivity coefficient $K_{A,B}^{\text{pot}}$ is 0.10, the system is detecting 10 target anions for every 1 interferent.^{19,20}

After observing the Hofmeister effect and assessing trends based on bambus[6]juril affinity toward a series of representative anions, we next investigated the specific affinity toward HS⁻ over competitive anions. In the previous section, reported results were experimentally observed in solutions with non-competing piperazine-*N,N'*-bis-2-ethanesulfonic acid (PIPES) buffer. However, this selectivity evaluation involved the examination of HS⁻ affinity in the presence of competing anions. The buffer pH was adjusted to pH 8 to ensure sufficient HS⁻ and cysteine thiolate speciation for accurate evaluation of anion interaction with bambusuril receptors in chemFET sensors.

Selectivity experiments were designed to evaluate interferents of practical interest when attempting to use electrochemical sensors in HS⁻ detection applications. Chloride is similar in size to HS⁻, which is often an important factor in determining selectivity in host-guest chemistry and supramolecular interactions. Cysteine is a thiol-containing biomolecule that introduces a competing -SH group as well as a carboxylate functionality, which is also known to bind within bambusuril hosts. We screened both as interferents, since they should be among the most competitively-binding anions based on similarities to hydrosulfide.

In both cases, incorporation of *n*-butyl bambusuril resulted in a selectivity coefficient of less than one. Calculated selectivity coefficients were 0.4 for chloride, and 0.037 for cysteine. Selectivity coefficients less than one indicates preference for HS⁻ over both Cl⁻ and cysteine thiolate. We attribute the large preference for HS⁻ binding over cysteine to the size limit of the bambusuril binding cavity, and it is encouraging to note that the carboxylate motif in cysteine does not apparently interfere either, suggesting selectivity for HS⁻ over other biological carboxylates as well.

Conclusions

ChemFETs provide a useful approach to exploit supramolecular host-guest interactions between hydrophobic hosts and aqueous anion guest. Highlighting the utility of this platform, we have demonstrated that receptor-containing ChemFETs can be designed to bind HS⁻, which is often difficult to work with and characterize due to its toxicity and reactivity. Incorporation of selective ionophores into the gate oxide membrane of a ChemFET provides the ability to measure aqueous anion concentration in real time, facilitating direct comparison to other anions of interest. We found that incorporation of dodeca-*n*-butyl bambus[6]juril into the ChemFET gate membrane improved competitive HS⁻ selectivity over size-similar Cl⁻, and thiol-containing cysteine. Further characterization of the bambus[6]juril ChemFETs against common anions in the Hofmeister series provided the relative affinity differences compared to the unaltered Hofmeister series arrangement. We found our electrochemical sensors to generally be more sensitive to charge diffuse chaotropes and generally less sensitive to charge dense kosmotropes. This trend held for both the control sensors as well as bambus[6]juril ionophore-containing sensors, with the ionophore further improving (or lowering) detection limits.

More broadly, our approach allowed for experimental validation of the previously reported theoretical calculations by Page and coworkers of HS⁻ placement in the Hofmeister series. Not only does this study serve to experimentally validate the Hofmeister placement of this one particular anion of interest, but it sets a precedent for the use of electrochemical sensors for similar types of benchmarking that may not be otherwise feasible due to challenges with synthesis, toxicity, reactivity, *etc.* Furthermore, these results provide an approach for designing an anion receptor with preferential binding for one particular target analyte over competing species based on tailored receptor



size and hydrogen bond donor configuration, which is well-known for cationic analytes but far less studied for their negatively charged counterparts.

Materials and methods

Electrode and membrane preparation

Silicon nitride-gated field effect transistors (FETs) were purchased from Winsense (<https://www.winsense.co.th>, WIPSC) and cleaned with ethanol and soaked in H₂O₂ for 10 minutes prior to functionalization. Polyvinyl chloride (PVC), 2-nitrophenyl octyl ether (NPOE), and tetraoctylammonium nitrate (TOAN) were obtained from Fisher Scientific and TCI Chemicals. Chemically sensitive membranes were deposited onto the FET surface by manual drop-casting. Four aliquots of 1.6 μ L dropcast solution were applied at 15 minute increments before being placed in an oven at 60 $^{\circ}$ C for at least 4 hours, yielding an approximate film thickness of 50 μ m. Polymer membrane dropcast solutions were formulated as follows:

Control sensor membranes:

- 66 wt% PVC (69.0 mg), 32 wt% NPOE (33.0 mg), and 2 wt% TOAN (2.0 mg) in THF (2 mL).

Bambusuril sensor membranes:

- 65 wt% PVC (68.6 mg), 32 wt% NPOE (33.2 mg), 2 wt% TOAN (2.0 mg), and 1 wt% dodeca-*n*-butyl bambus[6]juril (1.02 mg) in 50 : 50 anisole/THF (2 mL).

Ag/Ag₂S reference electrodes (REs) were used in measurements using NaSH, and Ag/AgCl REs are used in all other potentiometric experiments. All REs in this report were made in-house following previously-reported procedures.⁸

Synthetic procedures

Reagents and solvents were purchased from Fisher Scientific, Tokyo Chemical Industry or Sigma Aldrich. We note that NaSH and NH₄SH evolve H₂S gas in water and should be handled in a fume hood. Additionally, a Zn(OAc)₂ quench solution and a personal H₂S monitor are encouraged when there is potential for exposure outside of a glove box or fume hood. Scheme 1 outlines the synthesis the *N,N'*-dibutyl glycoluril and dodeca-*n*-butyl bambus[6]juril, which was adapted from literature.

4,5-Dihydroxyimidozoline (DHI, 1). 4,5-Dihydroxyimidozoline was synthesized according to literature procedure.²⁵

***N,N'*-Dibutyl glycoluril (*n*-butyl GLY, 2).** *N,N'*-Dibutylurea (2.39 g, 13.9 mmol) was added to a solution of 4,5-dihydroxyimidozoline (1.63 g, 13.8 mmol) in 35 mL of DI water.^{25,39} Concentrated hydrochloric acid (12.1 M, 1.1 mL) was added dropwise to the reaction mixture and stirred at reflux for 2 hours, at which point the reaction turned a cloudy yellow color. The reaction mixture was then cooled to room temperature and a light-yellow solid formed. The precipitate was collected *via* vacuum filtration and dried under vacuum. The crude product was dissolved in acetone and purified by column chromatography (SiO₂, 95 : 5 EtOAc : MeOH) to produce a fluffy white solid (1.54 g, 44%). ¹H NMR (500 MHz, DMSO-*d*₆) δ : 7.50 (s, 2H), 5.22 (s, 2H), 3.19 (m, 2H), 2.98 (m, 2H), 1.42 (m, 4H), 1.25 (m, 4H), 0.89 (t, *J* = 7.3 Hz, 6H).

Dodeca-*n*-butyl bambus[6]juril (dodeca-*n*-Bu BU[6], 3). Compound 2 (1.14 g, 4.40 mmol) was added to a mixture of paraformaldehyde (129 mg, 4.60 mmol) in 30 mL of 1,4-dioxane. While stirring, concentrated sulfuric acid (1 mL) was slowly added dropwise. The reaction mixture was heated at 80 $^{\circ}$ C for 1.5 hours. Upon heating, the reaction turned a clear light-yellow color, and darkened to an orange color as the reaction proceeded. Following the allotted time, the solution was cooled to room temperature and precipitation occurred. The precipitate was collected *via* vacuum filtration yielding an orange powder. The crude product was recrystallized in hot EtOH and acetonitrile (95 : 5 v/v) to yield colorless crystals (430 mg, 37% yield). Connectivity of the host structure was confirmed through a low resolution X-ray crystal structure (see ESI[†]), ¹H NMR (500 MHz, DMSO-*d*₆) δ : 5.44 (s, 2H), 4.80 (s, 2H), 3.44 (m, 4H), 1.50 (m, 4H), 1.23 (m, 4H), 0.86 (t, *J* = 7.3 Hz, 6H). ¹³C NMR (126 MHz, Chloroform-*d*) δ : 159.3, 159.1, 69.1, 48.7, 44.0, 30.2, 20.1, 13.9 and HRMS (ESI⁺): *m/z* calculated for [C₇₈H₁₃₂N₂₄O₁₂]: 1598.0636, found: 1598.0383 (see ESI[†]).

Potentiometric measurements

The ChemFETs were driven by a benchtop power source, and ISFETs obtained from Winsense were used as the device base. In operation, the drain voltage (*V*_{ds}) is held at 617.5 mV and the drain current (*I*_{ds}) at 100 mA. The external reference (Ag/AgCl or Ag/Ag₂S) is held at ground, and the voltage between ground and the source (*V*_{gs}) terminal changes to maintain the values of *V*_{ds} and *I*_{ds}. *V*_{gs} is recorded as the measurement signal. NI-DAQ 6009 at a rate of 1 kHz was used for data acquisition paired with a custom Labview program for collection. Hydrosulfide experiments employed 180 second measurement periods to minimize electrode fouling. The other potentiometric tests were recorded for 300 seconds.

Solutions used in these experiments were prepared and used at ambient temperature. Previously reported procedures were employed to prepare samples for hydrosulfide measurement.¹⁵ All solutions are based on a 50 mM PIPES buffer in DI water fixed to pH 7 using 4.0 M KOH. The hydrosulfide measurements were performed in pH 8 buffer to reduce H₂S release.⁸ Potassium or sodium salts containing the target anion were used to make 0.10 M stock solutions which were further diluted in 50 mL polypropylene centrifuge tubes for sensor calibration. Potassium was used as the counter cation for all evaluated analyte solutions (except for NaSH). To evaluate counter cation impact on anion sensitivity, a number of cations varying in formal charge, molecular geometry, and atomic radii were evaluated with a common counter anion (chloride) using ChemFET sensors. The results (ESI[†]) indicated none of the counter cations screened provided a statistically-significant impact to the relevant figures of merit in anion sensing. This information validated the reported anion sensing data between various salts. All reported results are the average of four sensors run in triplicate through the entire analyte solution series of 12 solutions spanning six orders of magnitude range of concentration.



Data availability

The datasets supporting this article have been uploaded as part of the ESI.†

Author contributions

The manuscript was written through contributions of all authors. Data were collected by Dr Grace Kuhl and Doug Banning, and all coauthors assisted with data analysis and interpretation. All authors have given approval to the final version of the manuscript.

Conflicts of interest

There are no conflicts to declare.

Acknowledgements

We thank the NIH (R21-GM129590 to D. W. J.) and the NSF (CHE-2107602 to M. D. P.) for support of this research. This work was also supported by the Bradshaw and Holzapfel Research Professorship in Transformational Science and Mathematics to D. W. J. and the Air Force Institute of Technology (D. H. B.).

Notes and references

§ Binding constants: the primary means of measuring host-guest interaction between dodeca-*n*-butyl bambus[6]uril with the target anions was *via* ChemFET evaluation and relative ranking of anions by respective detection limits. Although initial ¹H NMR titrations were performed to measure the binding constants of dodeca-*n*-butyl bambusuril with common halides, unfortunately many of the binding constants were too high to measure accurately using BindFit.⁴⁰ Thus, the lower bound of Cl⁻ K_a was estimated to be ~10⁷ M⁻¹ in CDCl₃. We also note that the similar dodecapropyl and dodecamethyl bambusurils were evaluated by Havel for solution state binding (Cl⁻, Br⁻, I⁻) using ¹H NMR titrations and isothermal titration calorimetry (ITC). Both techniques revealed the same Hofmeister trend when association constants were ranked: Cl⁻ < Br⁻ < I⁻.⁴¹

- P. Anzenbacher Jr, Y. Liu, M. A. Palacios, T. Minami, Z. Wang and R. Nishiyabu, *Chem.-Eur. J.*, 2013, **19**, 8497–8506.
- M. D. Hartle, R. J. Hansen, B. W. Tresca, S. S. Prakes, L. N. Zakharov, M. M. Haley, M. D. Pluth and D. W. Johnson, *Angew. Chem., Int. Ed.*, 2016, **55**, 11480–11484.
- Y. Jiang, D. Jin, Y. Li, X. Yan and L. Chen, *Res. Chem. Intermed.*, 2017, **43**, 2945–2957.
- V. Havel, M. Arfan Yawer and V. Sindelar, *Chem. Commun.*, 2015, **51**, 4666–4669.
- M. D. Hartle and M. D. Pluth, *Chem. Soc. Rev.*, 2016, **45**, 6108–6117.
- N. Lau, L. N. Zakharov and M. D. Pluth, *Chem. Commun.*, 2018, **54**, 2337–2340.
- J. Vázquez and V. Sindelar, *Chem. Commun.*, 2018, **54**, 5859–5862.
- T. J. Sherbow, G. M. Kuhl, G. A. Lindquist, J. D. Levine, M. D. Pluth, D. W. Johnson and S. A. Fontenot, *Sens. Bio-Sens. Res.*, 2021, **31**, 100394.
- X. Shen, E. A. Peter, S. Bir, R. Wang and C. G. Kevil, *Free Radicals Biol. Med.*, 2012, **52**, 2276–2283.
- E. J. Mitchell, A. J. Beecroft, J. Martin, S. Thompson, I. Marques, V. Félix and P. D. Beer, *Angew. Chem.*, 2021, **133**, 24250–24255.
- V. S. Lin, W. Chen, M. Xian and C. J. Chang, *Chem. Soc. Rev.*, 2015, **44**, 4596–4618.
- G. K. Kolluru, X. Shen, S. C. Bir and C. G. Kevil, *Nitric Oxide*, 2013, **35**, 5–20.
- L. Li, P. Du, Y. Zhang, Y. Duan, Y. Li, Y. Qian, P. Zhang and Q. Guo, *Sens. Actuators, B*, 2021, **345**, 130413.
- S. Berchmans, T. B. Issa and P. Singh, *Anal. Chim. Acta*, 2012, **729**, 7–20.
- P. E. Martín Vázquez, F. Brunel and J.-M. Raimundo, *ACS Omega*, 2020, **5**, 4733–4742.
- N. A. Chaniotakis, Y. Alifragis, G. Konstantinidis and A. Georgakilas, *Anal. Chem.*, 2004, **76**, 5552–5556.
- F. M. Abdel-Haleem and M. S. Rizk, *J. Adv. Res.*, 2017, **8**, 449–454.
- M. M. G. Antonisse and D. N. Reinhoudt, *Electroanalysis*, 1999, **11**, 1035–1048.
- J. Bobacka, A. Ivaska and A. Lewenstam, *Chem. Rev.*, 2008, **108**, 329–351.
- M. Kaisti, *Biosens. Bioelectron.*, 2017, **98**, 437–448.
- G. A. Crespo, *Electrochim. Acta*, 2017, **245**, 1023–1034.
- E. A. Moschou and N. A. Chaniotakis, *Mikrochim. Acta*, 2001, **136**, 205–209.
- C.-S. Lee, S. K. Kim and M. Kim, *Sensors*, 2009, **9**, 7111–7131.
- G. E. K. K. Seah, A. Y. X. Tan, Z. H. Neo, J. Y. C. Lim and S. S. Goh, *Anal. Chem.*, 2021, **93**, 15543–15549.
- V. Havel, J. Svec, M. Wimmerova, M. Dusek, M. Pojarova and V. Sindelar, *Org. Lett.*, 2011, **13**, 4000–4003.
- V. Havel, M. Babiak and V. Sindelar, *Chem.-Eur. J.*, 2017, **23**, 8963–8968.
- V. Havel, T. Sadilová and V. Šindelář, *ACS Omega*, 2018, **3**, 4657–4663.
- P. Itterheimová, J. Bobacka, V. Šindelář and P. Lubal, *Chemosensors*, 2022, **10**, 115.
- P. Jungwirth and P. S. Cremer, *Nat. Chem.*, 2014, **6**, 261–263.
- K. P. Gregory, G. R. Elliott, H. Robertson, A. Kumar, E. J. Wanless, G. B. Webber, V. S. J. Craig, G. G. Andersson and A. J. Page, *Phys. Chem. Chem. Phys.*, 2022, **24**, 12682–12718.
- W. J. Xie and Y. Q. Gao, *J. Phys. Chem. Lett.*, 2013, **4**, 4247–4252.
- C. L. D. Gibb, E. E. Oertling, S. Velaga and B. C. Gibb, *J. Phys. Chem. B*, 2015, **119**, 5624–5638.
- J. F. Neal, A. Saha, M. M. Zerkle, W. Zhao, M. M. Rogers, A. H. Flood and H. C. Allen, *J. Phys. Chem. A*, 2020, **124**, 10171–10180.
- K. P. Gregory, E. J. Wanless, G. B. Webber, V. S. J. Craig and A. J. Page, *Chem. Sci.*, 2021, **12**, 15007–15015.
- K. Wojciechowski and K. Linek, *Electrochim. Acta*, 2012, **71**, 159–165.
- K. Wojciechowski, M. Kucharek, W. Wróblewski and P. Warszyński, *J. Electroanal. Chem.*, 2010, **638**, 204–211.



- 37 H. A. Fargher, N. Lau, H. C. Richardson, P. H.-Y. Cheong, M. M. Haley, M. D. Pluth and D. W. Johnson, *J. Am. Chem. Soc.*, 2020, **142**, 8243–8251.
- 38 H. A. Fargher, T. J. Sherbow, M. M. Haley, D. W. Johnson and M. D. Pluth, *Chem. Soc. Rev.*, 2022, **51**, 1454–1469.
- 39 S. L. Vail, R. H. Barker and P. G. Mennitt, *J. Org. Chem.*, 1965, **30**, 2179–2182.
- 40 *BindFit*, <https://www.supramolecular.org>.
- 41 V. Havel, *Bambusuril Derivatives: Synthesis and Supramolecular Properties*, PhD dissertation, Masaryk University, Brno, Czech Republic, 2017.

